ISSN 0208-7774 TRIBOLOGIA 5/2018 p. 109–115

Katarzyna STRZELCZAK[*], Agata DUDEK[**]

THE STRUCTURE AND COEFFICIENT OF FRICTION OF WELDED NICKEL ALLOYS INCONEL 625 AND INCONEL 718

STRUKTURA I WSPÓŁCZYNNIK TARCIA SPAWANYCH POŁĄCZEŃ STOPÓW NIKLU INCONEL 625 I INCONEL 718

Key words: friction coefficient, friction force, Scratch Tester, hardness, heat treatment, Inconel 625, Inconel 718, electron beam welding.

Abstract

In this study, the coefficients of friction for three series of welded nickel alloy joints, subjected to different heat treatments (lack of heat treatment, solution heat treatment, precipitation hardening), were determined. Heat treatment of the prepared samples was aimed at eliminating the structural and stress gradient, because the electron beam welding technique is dedicated for constructions with very high quality and strength requirements. Given the nature of the electron beam process, the authors are aware that the obtained weld's structures are characterized by different properties from parent materials, and also from structures melted under equilibrium conditions.

The scientific aim of the presented work is to determine the influence of heat treatment on the microstructure, mechanical properties, and performance of dissimilar joints of nickel alloys Inconel 625 and Inconel 718. In order to determine the coefficient of friction for samples, the scratch test method was used.

As a result of the research, it was proved that subjecting the welds to the precipitation hardening has a significant effect on abrasion resistance.

Słowa kluczowe: współczynnik tarcia, siła tarcia, Scratch Tester, twardość, obróbka cieplna, Inconel 625, Inconel 718, spawanie wiązką elektronów.

Streszczenie

Wyznaczono współczynniki tarcia dla trzech serii próbek poddanych odmiennym procesom obróbki cieplnej (brak obróbki cieplnej, przesycanie, utwardzanie wydzieleniowe). Obróbka cieplna przygotowanych próbek miała na celu zlikwidowanie gradientu strukturalnego i naprężeniowego, ponieważ spawanie wiązką elektronów dedykowane jest dla urządzeń o bardzo wysokich wymaganiach jakościowych i wytrzymałościowych. Biorąc pod uwagę charakter procesu spawania wiązką, autorzy mają świadomość, iż uzyskane struktury będą cechowały się zdecydowanie odmiennymi własnościami od materiału rodzimego, ale również i od struktur przetopionych w warunkach bliskich warunkom równowagowym.

Celem naukowym pracy jest określenie wpływu obróbki cieplnej na mikrostrukturę, własności mechaniczne i użytkowe różnoimiennych połączeń stopów niklu Inconel 625 oraz Inconel 718. W celu wyznaczenia współczynników tarcia dla próbek zastosowano metodę zarysowania scratch test.

W wyniku przeprowadzonych badań dowiedziono, że poddanie spoin procesowi utwardzania wydzieleniowego ma znaczący wpływ na odporność na ścieranie.

INTRODUCTION

The dynamically developing industrial sectors, such as the aerospace industry, the space industry, or the energy industry aim at increasing the efficiency and longer lifespan of components working in difficult operating conditions, such as high temperatures, aggressive environments, and reactions with gases, liquids, and solids. Therefore, materials that can operate in extreme conditions are still developed [**L. 1–3**].

Austenitic nickel alloys, such as Inconel 625 and Inconel 718, exhibit very good properties at high temperatures between 150–1500°C, in terms of strength, corrosion resistance, stress-rupture strength, resistance

[*] Czestochowa University of Technology, Faculty of Production Engineering and Materials Technology, al. Armii Krajowej 19, 42-200 Częstochowa, Poland, e-mail: strzelczak.katarzyna@wip.pcz.pl.

to thermal fatigue, and toughness. For this reason, this materials are widely used in aircraft-engine hot section components, aerospace structures, and liquid rocket components, including both cryogenic and high temperature operating environments in gas turbines, submarines, and nuclear reactors [**L. 4**].

The excellent performance of Inconel 625 and Inconel 718 are the result of the existence of precipitate strengthened elements, such as Nb, Al, and Ti, by which this alloys can be strengthened by γ′, γ″, and δ phases. The face centred cubic (FCC) structure γ′ phase (Ni_3(Al,Ti) is coherent with the γ-Ni solid-solution matrix. The γ′ phase precipitates only brings a slight additional strength to the alloy [**L. 5–8**].

The main hardening phase is body-centred tetragonal (BCT) metastable γ″ phase (Ni_3Nb). As demonstrated by Paulonis et al. the volume fraction of γ″ phase is approximately 15%, while the volume fraction of ă′ phase is 4% [**L. 9–10**]. If the alloys is exposed to long ageing time or to temperatures higher than 850°C, γ″ transforms into a stable orthorhombic δ phase (Ni_3Nb-δ). Since γ″ and δ have the same composition, the growth of the δ phase occurs to the corresponding depletion of the γ″ phase. The presence of the γ phase adversely affects the yield and tensile strengths of the alloys, but it has a beneficial effect on the rupture ductility, creep, and fatigue properties [**L. 11–13**]. In addition, an appropriate amount of δ on the grain boundary prevents undesired grain growth [**L. 14**]. The solidification process of cast or welded nickel alloys is related to the segregation of elements such as Nb and Mo, which results in the formation of the Laves phase $(Ni, Cr, Fe)_2$ (Nb, Mo, Ti). The Laves phase is a brittle intermetallic compound that often forms at the interdendritic regions [**L. 15**]. Moreover, the presence of this phase has the effect of the deterioration of the material tensile ductility, fatigue, and creep-rupture properties [**L. 16–17**]. In order to minimize the segregation of niobium and the Laves phase in the fusion zone of welded Inconels®, increasing the cooling rates of welded alloys are necessary [**L. 18**], and it depends on the type of welding technique, which controls heat input and dictates liquid metal convection in the weld pool [**L. 19–20**].

The scope of this study is to investigate the effect of heat treatment of dissimilar joints on the microstructure, the values of the coefficient of friction, and hardness of the nickel alloys.

MATERIAL AND METHODS

In order to prepare specimens for research, sheets of Inconel 625 and Inconel 718 were subjected to the operations described in **Table 1**. The chemical composition of nickel alloys is presented in **Fig. 1**.

Table 1. Methodology for the creation of specimens for research
Tabela 1. Metodyka wytworzenia próbek do badań

Name of the specimens	
A0	I STAGE: solution heat treatment of Inconel 718; 954°C/1h II STAGE: electron beam welding of Inconel 718 and Inconel 625 with filler material III STAGE: no heat treatment
A1	I STAGE: solution heat treatment of Inconel 718; 954°C/1h II STAGE: electron beam welding of Inconel 718 and Inconel 625 with filler material III STAGE: solution heat treatment; 954 °C/1h
A2	I STAGE: solution heat treatment of Inconel 718; 954°C/1h II STAGE: electron beam welding of Inconel 718 and Inconel 625 with filler material III STAGE: solution heat treatment 954°C/1h, and then two-stage aging: first 718°C/8h and then 621°C/8h

The etching of joints was carried out with a mixture of 4 g $CuSO_4$, 20 ml HCl, 1 ml H_2SO_4, and distilled water. Microstructure examinations of the Inconel 625-Inconel 718 joints were carried out using a Jeol JSM-6610 LV scanning electron microscope with an EDX analyser and optical microscope OLYMPUS GX41. In order to compare the mechanical properties of the initial sample (A0) and heat treated samples after welding (A1 and A2), a Vickers microhardness tester, Shimadzu HMV-G -21DT, with load of 980.7 mN was used. The average hardness for each of weld joints in each of the specimens was determined. In order to determine the kinetics coefficient of the friction of welds, a scratch test was performed using a Revetest Xpress Scratch Tester. A schematic diagram of scratch tests is presented in **Fig. 1**. The indenter cone was Rockwell made of diamond with radius of 200 μm. The indenter velocity of 0.3 mm/min was used over a wear tracks of 5 mm. Constant Load Scratch Test (CLST) mode of scratch testing was used. The normal load was constant during the tests and amounted to 100 N.

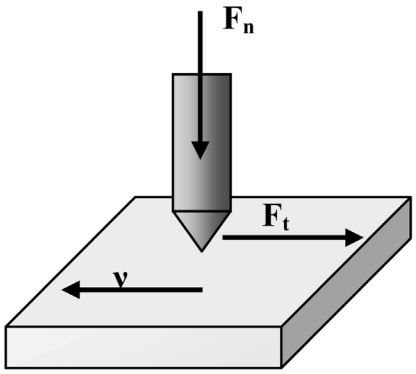

Fig. 1. Schematic diagram of scratch test
Rys. 1. Schematyczny rysunek testu zarysowania

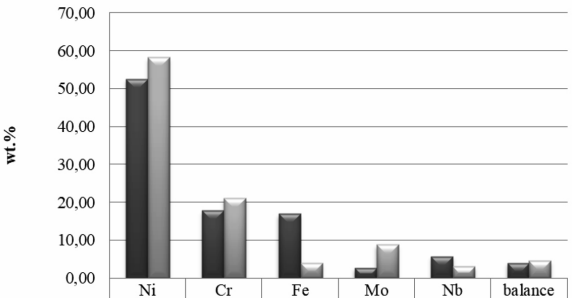

	Ni	Cr	Fe	Mo	Nb	balance
Inconel 718	52,55	17,85	17,00	2,78	5,80	4,02
Inconel 625	58,27	21,17	4,06	8,82	3,07	4,61

Fig. 2. Chemical composition of nickel alloys Inconel 718 and Inconel 625
Rys. 2. Skład chemiczny stopów niklu Inconel 718 i Inconel 625

RESULTS AND DISSCUSION

Microstructural examinations concurred that the weldments obtained from the electron beam welding technique were free from surface or sub-surface flaws including porosity, upset metal, spatter, and under-cuts (**Fig. 3**).

A narrow heat affected zone (HAZ) is observed for all weld joints, which is characteristic for the electron beam welding technique. Such a narrow heat affected zone is possible due to the strong concentration and high stability of the electron stream, which means that the total heat input is much lower than in other welding technologies. Microstructures at the fusion zones showed the presence of the dendritic structures of each weldment. A microstructure of the fusion zone of A1 specimen showed the presence of fine equiaxed dendrites, and the fusion zone of A0 and A2 specimens exhibited coarse dendrites. In **Fig. 4**, the microstructure of fusion zones of samples A0, A1, and A2 are presented. In each case (**Figs. 4a-i**), the distribution of the individual phases is consistent with the direction of the heat outflow. In comparison to the weld microstructure A0 (**Figs. 4a-c**), a second operation of the solution heat treatment of Sample A1 (**Figs. 4d-f**) resulted in coagulation and change in the morphology of the precipitates. However, the use of the precipitation hardening process after electron beam welding (**Figs. 4g-i**) led to quantitative and qualitative changes in the precipitates.

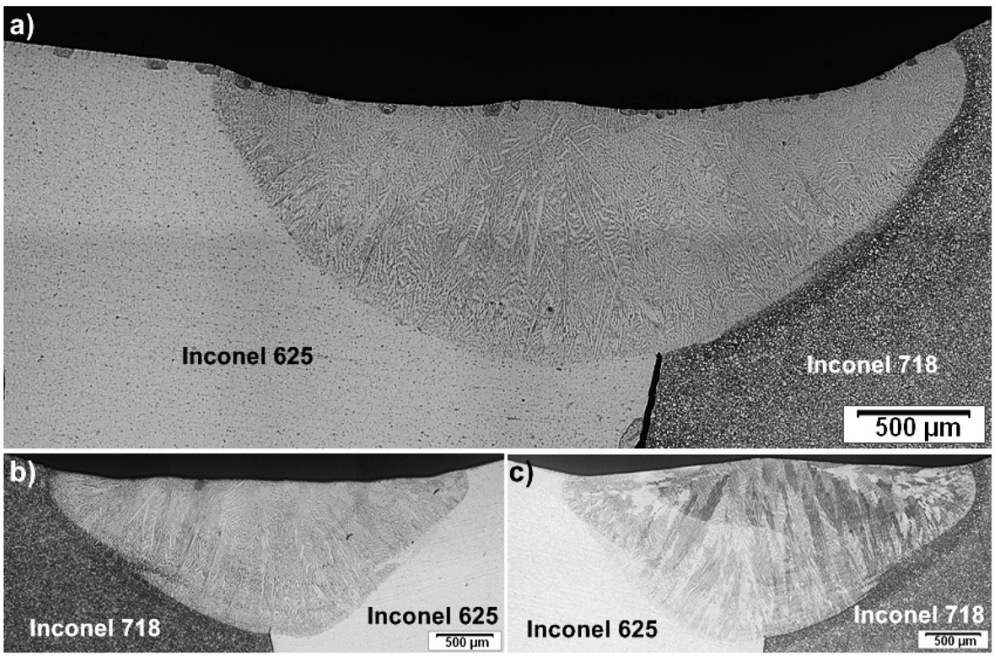

Fig. 3. Microstructure of weld joints: a) A0, b) A1, and c) A2
Rys. 3. Mikrostruktura połączeń spawanych: a) A0 c) A1 c) A2

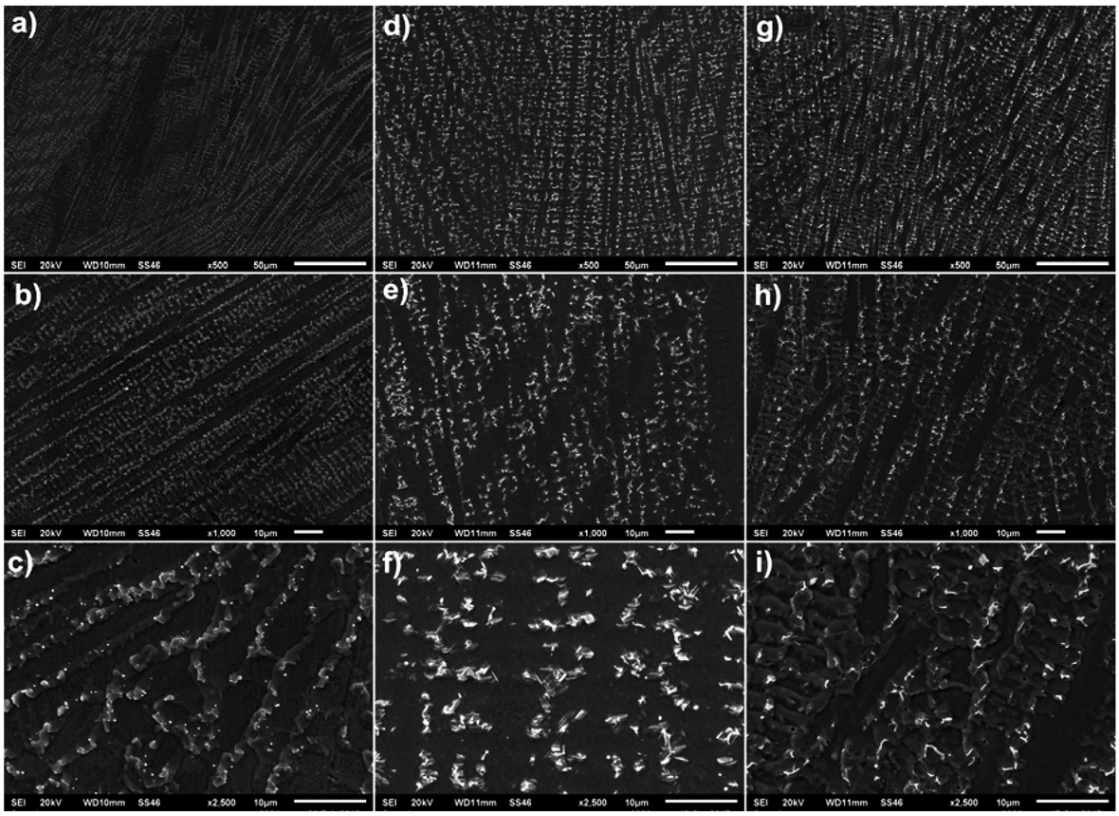

Fig. 4. SEM images of microstructure of fusion zone of a,b,c of Sample A0, d,e,f of Sample A1, and g,h,i of Sample A2
Rys. 4. Obrazy SEM mikrostruktury strefy przetopienia a, b, c – próbki A0, d, e, f – próbki A1, g, h, i – próbki A2

Microhardness measurements (**Fig. 5**) showed that, regardless of what operations the structural elements have been subjected to, Inconel 718 has the highest hardness value, while dissimilar joints show intermediate hardness values between base materials. The weld joint not subjected to any heat treatment after electron beam welding process (Sample A0) exhibits the lowest hardness value (247 HV0.1). Application of second solution heat treatment led to slight increase in the hardness of Sample A1 compared to Sample A0, and Sample A2, and only the aging process forms the performance properties of Samples A2 (374 HV0.1).

The results of scratch test are shown in **Figs 6, 7**, and **8**. As a result of the test, it was shown that precipitation strengthening dissimilar joint (Sample A2) has the lowest (0.33) and as-welded joint (Sample A0) has the highest coefficient of friction (0.39). The above correlations are confirmed by the results of hardness tests for fusion zones.

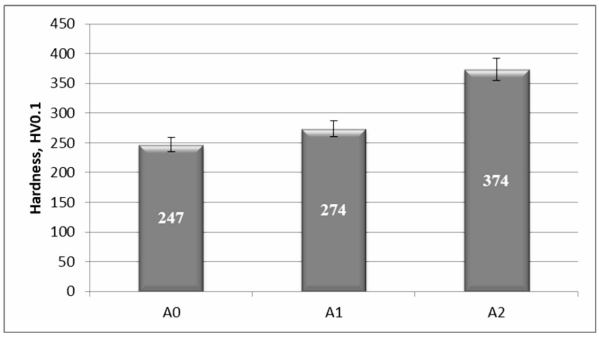

Fig. 5. Average hardness of joints of Inconel 625 – Inconel 718
Rys. 5. Średnia wartość twardości dla materiałów dla połączeń spawanych Inconel 625 – Inconel 718

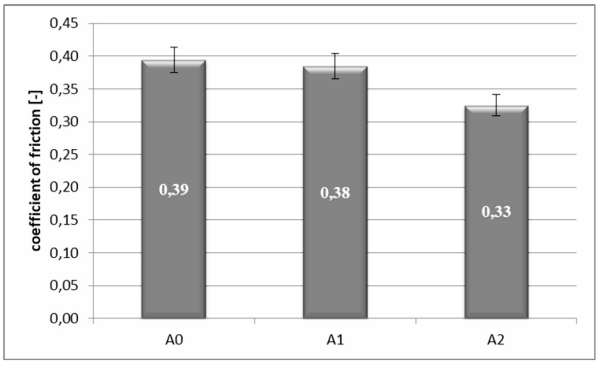

Fig. 6. Coefficient of friction of joints of Inconel 625 – Inconel 718
Rys. 6. Współczynnik tarcia połączeń spawanych Inconel 625 – Inconel 718

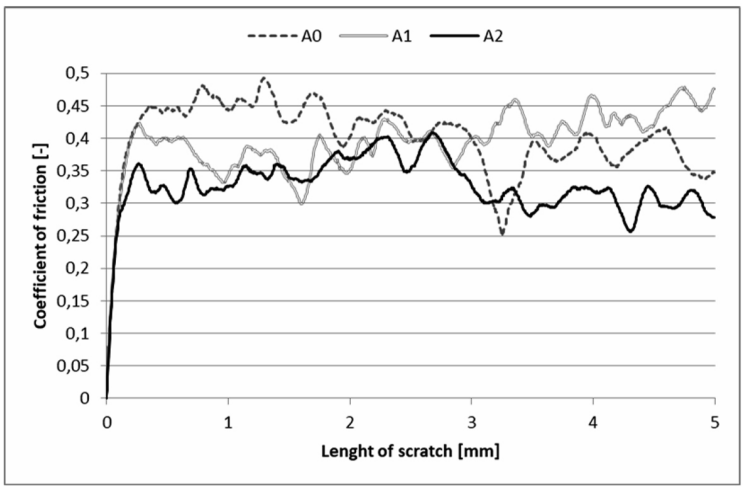

Fig. 7. Coefficient of friction as a function of road for A0, A1 and A2 joints
Rys. 7. Współczynnik tarcia w funkcji drogi dla złącz A0, A1 i A2

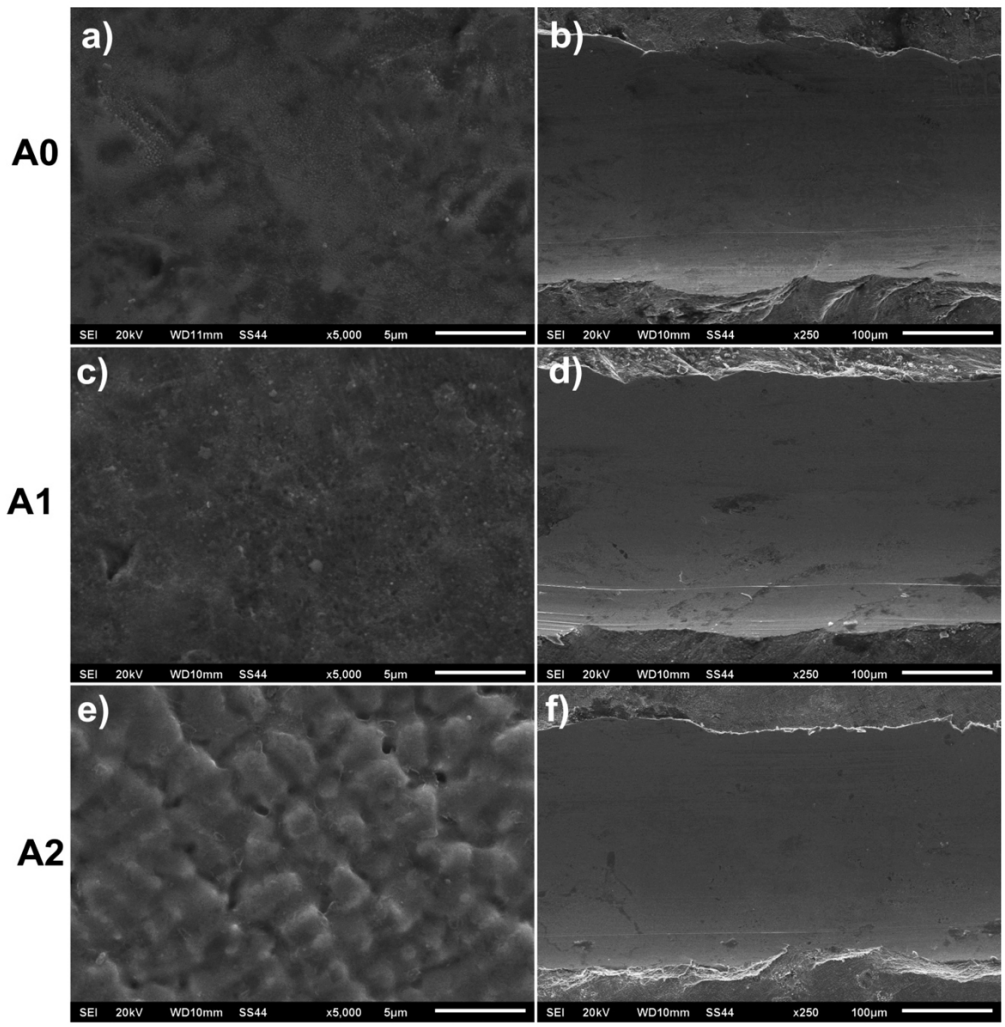

Fig. 8. Topography of the surface of welds of Sample A0, A1, and A2 (Figs. a, c, e) and the surface of the welds after scratch with diamond intender (Figs b, d, f).
Rys. 8. Topografia powierzchni spoin próbek A0, A1, A2 (**Rys. a, c, e**) oraz powierzchni spoiny po zarysowaniu diamentowym wgłębnikiem (**Rys. h, d, f**)

Figure 8 shows the topography of the weld surface before and after scratching. Scratching of the weld of Sample A2 is characterized by the smallest width value. Simultaneously, small surface development of Sample A2 scratching is observable compared to the scratches of A0 and A1 welds, which correlate with values of the coefficient of friction and hardness.

CONCLUSIONS

The intention of the present study was to determine the impact of dissimilar weld joints of Inconel 718 and Inconel 625 on the performance of the resulting structural element in the perspective of expanding the use of weld joints of these materials. On the basis of the performed tests, the following conclusions can be drawn:

- The dissimilar weldments obtained from the electron beam welding technique were free from surface or sub-surface flaws including porosity, upset metal, spatter, and under-cuts.
- The fusion zones of each sample showed the presence of dendritic structure. The microstructure of fusion zone of solution heat treatment sample (A1) showed the presence of finer equiaxed dendrites than Samples A2 and A0.
- The operation of solution heat treatment of the weld after electron beam welding caused a coagulation and change of the morphology of the precipitates. On the other hand, the change of the weld microstructure, which took place as a result of the precipitation hardening process, resulted in the improvement of strength properties and resistance to abrasive wear.

REFERENCES

1. Song G., Sun Z., Poplawsky J.D., Gao Y., Liaw P.K.: Microstructural evolution of single Ni_2TiAl or hierarchical NiAl/Ni2TiAl precipitates in Fe-Ni-Al-Cr-Ti ferritic alloys during thermal treatment for elevated-temperature applications. Acta Materialia, 2017, vol. 127, pp. 1–16.
2. Verdi D., Garrido M.A., Múnez C.J., Poza P.: Influence of exposure at high temperature on the local scratch mechanisms in laser cladded Inconel 625-base metal matrix composite coatings. Journal of Alloys and Compounds, 2018, vol. 733, pp. 69–81.
3. Feng K., Chen Y., Deng P., Li Y., Zhao H., Fenggui L., Li R., Huang J., Li Z.: Improved high-temperature hardness and wear resistance of Inconel 625 coatings fabricated by laser cladding. Journal of Materials Processing Technology, 2017, vol. 243, pp. 82–91.
4. Ramkumar K.D., Abraham W.S., Viyash V., Arivazhagan N., Rabel A.M.: Investigations on the microstructure, tensile strength and high temperature corrosion behavior of Inconel 625 and Inconel 718 dissimilar joints. Journal of Manufacturing Processes, 2017, vol. 25, pp. 306–322.
5. You X., Tan Y., Zhao L., You Q., Wang Y., Ye F., Li J.: Effect of solution heat treatment on microstructure and electrochemical behavior of electron beam smelted Inconel 718 superalloy. Journal of Alloys and Compounds, 2018, vol. 741, pp. 792–803.
6. Cao G.H., Sun T.Y., Wang C.H., Li X., Liu M., Zhang Z.X., Hu P.F., Russel A.M., Schneider R., Gerthsen D., Zhou Z.J., Li C.P., Chen G.F.: Investigations of γ', γ'' and δ precipitates in heat-treated Inconel 718 alloy fabricated by selective laser melting. Materials Charakterizatation, 2018, vol. 136, pp. 398–406.
7. You X., Tan Y., Shi S., Yang J.M., Wang Y., Li J., You Q.: Effect of solution heat treatment on the precipitation behavior and strengthening mechanisms of electron beam smelted Inconel 718 superalloy. Materials Science & Engineering A, 2017, vol. 689, pp. 257–268.
8. Deng D., Wang C., Liu Q., Niu T.: Effect of standard heat treatment on microstructure and properties of borided Inconel 718. Transactions of Nonferrous Metals Society of China, 2015, vol. 25, pp. 437–443.
9. Paulonis D.F., Oblak J.J., Duvall D.S.: Precipitation in nickel-base alloy 718. Technical report 1969, Pratt&Whitney Aircraft, Middletown, Conn.
10. Yadav P.C., Sahu S., Subramaniam A., Shekhar S.: Effect of heat-treatment on microstructural evolution and mechanical behaviour of severely deformed Inconel 718. Materials Science & Engineering A, 2018, vol. 715, pp. 295–306.
11. Anderson M., Thielin A.-L., Bridier F., Bocher P., Savoie J.: δ phase precipitation in Inconel 718 and associated mechanical properties. Materials Science & Engineering A, 2017, vol. 679, pp. 48–55.
12. Sundararaman M., Mukopadhyay P., Banerjee S.: Precipitation of the δ-Ni_3Nb phase in two nickel base superalloys. Metallurgical Transactions A, 1988, vol. 19., pp. 453–465.
13. Cai D., Zhang W., Nie P., Liu W., Yao M.: Dissolution kinetics of ä phase and its influence on the notch sensitivity of Inconel 718, 2007, vol. 58, pp. 220–225.

14. Deng D., Peng R.L., Brodin H., Moverare J.: Microstructure and mechanical properties of Inconel 718 produced by selective laser melting: Sample orientation dependence and effects of post heat treatments, Materials Science & Engineering A, 2018, vol. 713, pp. 294–306.
15. Xing X., Di X., Wang B.: The effect of post-weld heat treatment temperature on the microstructure on Inconel 625 deposited metal. Journal of Alloys and Compounds, 2014, vol. 593, pp. 110–116.
16. Tucho W.M., Cuvillier P., Sjolyst-Kverneland A., Hansen V.: Microstructure and hardness studies of Inconel 718 manufactured by selective laser melting before and after solution heat treatment. Materials Science & Engineering A, 2017, vol. 689, pp. 220–232.
17. Xu F., Lv Y., Liu Y., Xu B., Ge P.: Effect of heat treatment on microstructure and mechanical properties of Inconel 625 alloy fabricated by pulsed plasma arc deposition. Physics Procedia, 2013, vol. 50, pp. 48–54.
18. Reddy M.G., Srinivasa Murthy C.V., Rao S., Prasad Rao K.: Improvement of mechanical properties of Inconel 718 electron beam welds – influence of welding techniques and postweld heat treatment.The International Journal of Advanced Manufacturing Technology, 2009, vol. 43, pp. 671–680.
19. Biswas S., Reddy G.M., Mohandas T., Murthy C.V.S.: Residual stresses in Inconel 718 electron beam welds. Journal of Materials Science, 2004, vol. 39, pp. 6813–6815.
20. Radhkrishna C.H., Prasad Rao K.: The formation and control of Laves phase in superalloy 718 welds. Journal of Materials Science, 1997, vol. 32, pp. 1977–1984.